# Towards a More General Many-Objective Evolutionary Optimizer using Multi-Indicator Density Estimation

Jesús Guillermo Falcón-Cardona
Computer Science Department
CINVESTAV-IPN
Mexico, Mexico City 07360
jfalcon@computacion.cs.cinvestav.mx

Carlos A. Coello Coello
Computer Science Department
CINVESTAV-IPN
Mexico, Mexico City 07360
ccoello@cs.cinvestav.mx

## ABSTRACT

Recently, it was shown that Many-Objective Evolutionary Algorithms (MaOEAs) that employ a set of convex weight vectors are overspecialized in solving certain benchmark problems. This overspecialization is due to a high correlation between the Pareto fronts of the test problems and the simplex formed by the weight vectors. In furtherance of avoiding this issue, we propose a novel steady-state MaOEA that does not require weight vectors and adaptively chooses between two density estimators: one based on the IGD$^+$ indicador that strengthens convergence to the Pareto front and another one, based on the s-energy indicator, which improves the diversity of the solutions. This approach, called sIGD$^+$-MOEA, is compared with respect to NSGA-III, MOEA/D, IGD$^+$-EMOA and MOMBI2 (which are MaOEAs that employ convex weight vectors) on the test suites WFG and WFG$^{-1}$, using the hypervolume indicator. Experimental results show that sIGD$^+$-MOEA is a promising alternative that can solve many-objective optimization problems whose Pareto fronts present different geometries.

## CCS CONCEPTS

• **Theory of computation → Bio-inspired optimization**; • **Computing methodologies → Continuous space search**;

## KEYWORDS

Multi-objective Optimization, Quality Indicators, Adaptive Heuristics Selection

**ACM Reference Format:**
Jesús Guillermo Falcón-Cardona and Carlos A. Coello Coello. 2018. Towards a More General Many-Objective Evolutionary Optimizer using Multi-Indicator Density Estimation. In *GECCO '18 Companion: Genetic and Evolutionary Computation Conference Companion, July 15–19, 2018, Kyoto, Japan,* Jennifer B. Sartor, Theo D'Hondt, and Wolfgang De Meuter (Eds.). ACM, New York, NY, USA, 4 pages. https://doi.org/10.1145/3205651.3208221


*GECCO '18 Companion, July 15–19, 2018, Kyoto, Japan*

ACM ISBN 978-1-4503-5764-7/18/07…$15.00
https://doi.org/10.1145/3205651.3208221

## 1 INTRODUCTION

In this work, we focus on multi-objective optimization problems (MOPs) which involve the simultaneous optimization of several, often conflicting, objective functions of the form:

$$\min_{\vec{x}\in\Omega} \vec{F}(\vec{x}) = (f_1(\vec{x}), f_2(\vec{x}), \ldots, f_m(\vec{x}))^T, \tag{1}$$

where $\vec{x}$ is the vector of decision variables, $\Omega \subseteq \mathbb{R}^n$ is the decision variable space and $\vec{F}(\vec{x})$ is the vector of $m$ ($\geq 2$) objective functions ($f_i : \mathbb{R}^n \mapsto \mathbb{R}$) that belongs to the feasible objective space $\Psi \subseteq \mathbb{R}^m$. MOPs having four or more objective functions are called many-objective optimization problems (MaOPs) [9]. Solving a MOP involves finding the best possible trade-offs among its objectives. The particular set that yields the optimum values is known as the Pareto Optimal Set ($\mathcal{P}^*$) and its image in objective space is known as the Pareto Optimal Front ($\mathcal{PF}^*$).

Multi-Objective Evolutionary Algorithms (MOEAs) are metaheuristics based on the principles of natural selection. They are population-based and gradient-free search methods that have been successfully applied to solve complex MOPs [1]. Commonly, MOEAs have employed the Pareto dominance relation[1] as their main selection mechanism and a density estimator as secondary selection criterion in order to improve diversity. However, Pareto-based MOEAs do not perform properly when solving MaOPs due to the exponential increase of solutions preferred by the Pareto dominance relation which implies a dilution of the selection pressure [9]. Consequently, three main approaches have been proposed in order to design Many-Objective Evolutionary Algorithms (MaOEAs): (1) to use a set of reference points to guide the selection process, (2) decomposition of the MOP, and (3) the use of an indicator-based selection mechanism.

Most state-of-the-art MaOEAs employ a set of convex weight vectors. A vector $\vec{w} \in \mathbb{R}^m$ is a convex weight vector if $\sum_{i=1}^{m} w_i = 1$ and $w_i \geq 0$ for all $i = 1, \ldots, m$. These weight vectors lie on an $(m-1)$-simplex and are used by MaOEAs as search directions [11], reference points [2, 10] and as part of a quality indicator [5]. However, Ishibuchi *et al.* [8] empirically showed that the use of convex weight vectors overspecializes MaOEAs on MOPs whose Pareto fronts are strongly correlated to the simplex formed by such weight vectors. In other words, such MaOEAs are unable to produce good results when tackling MOPs whose Pareto fronts are not highly coupled with the $(m-1)$-simplex.

[1] A solution $\vec{x} \in \Omega$ Pareto-dominates a solution $\vec{y} \in \Omega$ (denoted as $\vec{x} \prec \vec{y}$), if and only if $\forall i \in \{1, \ldots, m\}, f_i(\vec{x}) \leq f_i(\vec{y})$ and $\exists j \in \{1, \ldots, m\} : f_j(\vec{x}) < f_j(\vec{y})$. In case, $f_i(\vec{x}) \leq f_i(\vec{y})$ for all $i \in \{1, \ldots, m\}$, $\vec{x}$ is said to weakly dominate $\vec{y}$ and it is denoted as $\vec{x} \preceq \vec{y}$.

In this work, we focus on tackling this overspecialization by proposing a MaOEA that benefits from the interaction/synergy between two indicator-based density estimators: one based on the IGD$^+$ indicator [7] which aims to drive the population to $\mathcal{PF}^*$ and another one, based on the s-energy indicator [4], which promotes the generation of uniformly distributed solutions. The proposed approach, called sIGD$^+$-MOEA, does not require a set of convex weight vectors in any of its mechanisms. Thus, it is a more general optimizer that can solve MOPs having different Pareto front geometries.

Quality indicators (QIs) are real-value functions that numerically assess aspects such as convergence, distribution and spread of an approximation to the Pareto front (denoted as $\mathcal{A}$) produced by an MOEA [13]. Regarding convergence QIs, a valuable property is Pareto-compliance. A (weakly) Pareto-compliant QI guarantees that one algorithm's indicator values are better (or at least not worse) than another in case the approximation sets of the former (weakly) dominates the other's. Hence, it is straightforward to think that if the indicator is optimized, we will obtain a better $\mathcal{A}$. Typically, Indicator-based MOEAs (IB-MOEAs) have been designed by a single QI. In consequence, their search behavior and produced approximation sets show characteristics related to the QI being used. However, an open research field is to determine which is the effect of a multi-indicator selection mechanism. sIGD$^+$-MOEA exploits this idea by combining two QIs. On the one hand, IGD$^+$, proposed by Ishibuchi *et al.* [7], is a convergence indicator that is weakly Pareto compliant. Mathematically, given an approximation set $\mathcal{A}$ and a reference set $\mathcal{Z}$, IGD$^+$ is defined as follows (assuming minimization):

$$\mathrm{IGD}^+(\mathcal{A}, \mathcal{Z}) = \frac{1}{|\mathcal{Z}|} \sum_{\vec{z} \in \mathcal{Z}} \min_{\vec{a} \in \mathcal{A}} d^+(\vec{a}, \vec{z}) \tag{2}$$

where $d^+(\vec{a}, \vec{z}) = \sqrt{\sum_{k=1}^{m} [\max a_k - z_k, 0]^2}$. IGD$^+$ measures the average distance from each reference vector to the nearest dominated region related to an element in $\mathcal{A}$. The aim is to minimize the value of IGD$^+$. On the other hand, Hardin and Saff proposed the s-energy indicator [4] in order to measure the even distribution of a set of points in $k$-dimensional manifolds. Its mathematical definition is given by the next formula:

$$E_s(\mathcal{A}) = \sum_{i \neq j} \left\| \vec{a}_i - \vec{a}_j \right\|^{-s} \tag{3}$$

where $\mathcal{A}$ is an approximation set which represents a manifold,[2] and $s > 0$ is a fixed parameter. Its minimization leads to a uniform distribution of the points in $\mathcal{A}$ if $s \geq k$ [4].

The remainder of this paper is organized as follows. Section 2 describes our proposed sIGD$^+$-MOEA. In Section 3, we present our experimental results using the Walking-Fish-Group (WFG) [6] test suite and its minus version WFG$^{-1}$. Finally, Section 4 provides our preliminary conclusions and some possible research paths.

[2] The Pareto front of a MOP with $m$ objective functions is at most an $(m-1)$-manifold. In case the dimension is less than $m-1$, the Pareto front is called degenerated.

## 2 OUR PROPOSED APPROACH

sIGD$^+$-MOEA is a steady-state MOEA that uses Pareto dominance as its main selection criterion and incorporates two indicator-based density estimators (IB-DEs) where each one is employed depending on certain conditions. An IB-DE requires two steps: (1) calculate the individual contributions to the indicator of each solution, (2) delete the worst-contributing solution. For IGD$^+$, the individual contribution $C$ of a solution $\vec{a} \in \mathcal{A}$ is defined as follows: $C(\vec{a}, \mathcal{A}, \mathcal{Z}) = |\mathrm{IGD}^+(\mathcal{A}, \mathcal{Z}) - \mathrm{IGD}^+(\mathcal{A} \setminus \{\vec{a}\}, \mathcal{Z})|$. Regarding s-energy, the individual contribution of $\vec{a} \in \mathcal{A}$ is given by: $C(\vec{a}, \mathcal{A}) = \frac{1}{2}\left(E_s(\mathcal{A}) - E_s(\mathcal{A} \setminus \{\vec{a}\})\right)$. Based on these equations and the above steps, we define the density estimators: IGD$^+$-DE and S-ENERGY-DE, respectively.

Through the search process, sIGD$^+$-MOEA switches between IGD$^+$-DE and S-ENERGY-DE depending on the quality of the population measured by an approximation to the hypervolume indicator [12] (denoted as $HV_{appr}$). At the end of each generation, $HV_{appr}$ is computed and the value is stored in a circular array $S_{\mathrm{HV}}$ of size $T_w$. After the first $T_w$ generations, we calculate the index of distribution $\beta$ of the samples and a linear regression model is computed in order to determine the angle $\theta$ related to the slope of the linear model. Using $\beta$ and $\theta$ and the thresholds $\bar{\beta}$ and $\bar{\theta}$, we can determine if sIGD$^+$-MOEA has stagnated regarding the convergence graph produced by $HV_{appr}$. If the search process is stagnated, we execute S-ENERGY-DE in order to improve diversity; otherwise, we employ IGD$^+$-DE.

**Algorithm 1** sIGD$^+$-MOEA general framework

**Require:** $T_w, \bar{\beta}, \bar{\theta}$
**Ensure:** Pareto front Approximation

```
Randomly initialize population P
r ← 0
while stopping criterion is not fulfilled do
    q ← Variation(P)
    Q ← P ∪ {q}
    {L_1, L_2, ..., L_k} ← nondominated-sorting(Q)
    Update reference point z^max using L_1
    S_HV[r mod T_w] ← HV_appr(L_1, z^max)
    Statistically analyze the last T_w samples in S_HV and generate β and θ
    if k = 1 and β ≤ β̄ and θ ∈ [−θ̄, θ̄] then
        c ← S-ENERGY-DE(L_1, m)
        j ← arg max_i c_i
    else
        if |L_k| > 1 then
            Z ← L_1
            c ← IGD+-DE(L_k, Z)
            j ← arg min_i c_i
        else
            j is equal to the sole individual in L_k
    P ← Q \ {j}
    r ← r + 1
return P
```

In Algorithm 1, we present the pseudocode of sIGD$^+$-MOEA. It requires three parameters: $T_w, \bar{\beta}$ and $\bar{\theta}$. Since our proposed approach is a steady-state MOEA, it generates one offspring per generation

**Table 1: Parameters adopted in our experiments.**

| | | | | | | |
|---|---|---|---|---|---|---|
| Objectives ($m$) | | 2 | 3 | 4 | 5 | 6 |
| Population size | | 120 | 120 | 120 | 126 | 126 |
| Objective function evaluations ($\times 10^3$) | | 50 | 50 | 60 | 70 | 80 |
| WFG | variables ($n$) | 24 | 26 | 28 | 30 | 32 |
| | position-related parameters | 2 | 2 | 3 | 4 | 5 |
| Weight-vector partitions ($H$) | | 119 | 14 | 7 | 5 | 4 |

(line 4). This newly created solution is added to the current population $P$ in order to form the temporary population $Q$. $Q$ is ranked by the nondominated sorting algorithm [2] in order to form the ranks $\{L_1, L_2, \dots, L_k\}$, where $L_1$ is the set of nondominated solutions and $L_k$ represents the worst solutions regarding Pareto dominance. In line 8, $HV_{appr}$ is calculated using $L_1$ and the value is stored in $S_{\mathrm{HV}}$. The statistical analysis of $S_{\mathrm{HV}}$ is done in line 9 in order to compute $\beta$ and $\theta$. Based on these values, sIGD$^+$-MOEA decides which IB-DE to execute.

## 3 EXPERIMENTAL RESULTS

In order to illustrate the efficiency of sIGD$^+$-MOEA, we focus on WFG2 and WFG6 as well as on their minus versions: WFG2$^{-1}$ and WFG6$^{-1}$ (the complete study is available at [3]) for 2 to 6 objective functions. We compare the results of sIGD$^+$-MOEA with respect to IGD$^+$-EMOA[3] [10], NSGA-III[4] [2], MOEA/D[5] [11] and MOMBI2[6] [5]. All common adopted parameter values used by the selected MOEAs and our proposed approach are described in Table 1. Regarding sIGD$^+$-MOEA, the values of $\bar{\beta}$ and $\bar{\theta}$ were set to 0.01 and 0.25°, respectively for all the test instances. The neighborhood size $T$ of MOEA/D was set to 20 in all cases. Since our proposed approach and the considered MOEAs employ Simulated Binary Crossover (SBX) and polynomial-based mutation (PBX) as their variation operators, for two and three objective functions, the crossover probability and distribution index were set to 0.9 and 20, respectively; while for MaOPs, these values were set to 1.0 and 30. For PBX, the probability and distribution index were set to $1/n$ and 20, respectively. For performance assessment of the MOEAs, we used the hypervolume indicator (HV), and its reference point was set to $\{2*i+1\}_{i=1,2,\dots,m}$. We performed 30 independent runs for all scenarios, and we applied the Wilcoxon rank sum test (one-tailed) to the mean hypervolume indicator values in order to determine whether sIGD$^+$-MOEA performed better than the other MOEAs at the significance level of 5%. In Tables 2 and 3, the two best HV values are highlighted using gray tones where the darker one corresponds to the best HV value. The symbol # is placed when sIGD$^+$-MOEA performs better in a statistical signficant way.

Table 2 presents the hypervolume values for the problems WFG2 and WFG6. Clearly, sIGD$^+$-MOEA was unable to obtain the best results. However, the differences concerning the best MOEA are not very significant. Overall, our approach obtains the third place in the ranking of MOEAs. Figure 1 shows the Pareto fronts for WFG6 of all MOEAs adopted in our study. Based on these plots, it is possible to see that the HV differences are due to the distribution of solutions.

[3]The source code was provided by its author Edgar Manoatl Lopez.
[4]Available at http://web.ntnu.edu.tw/~tcchiang/publications/nsga3cpp/nsga3cpp.htm
[5]Available at http://dces.essex.ac.uk/staff/zhang/webofmoead.htm
[6]EMO Project available at http://computacion.cs.cinvestav.mx/~rhernandez/

**Table 2: Mean and standard deviation (in parentheses) of the hypervolume indicator for the compared MOEAs and sIGD$^+$-MOEA in WFG2 and WFG6**

| MOP | Dim. | sIGD$^+$-MOEA | IGD$^+$-EMOA | NSGA-III | MOEA/D | MOMBI2 |
|---|---|---|---|---|---|---|
| WFG2 | 2 | 1.097554e+01 (4.122132e-01) | 1.100954e+01 (3.978609e-01) | 1.091544e+01# (3.990434e-01) | 9.812547e+00# (5.469032e-01) | 1.076660e+01# (3.822806e-01) |
| | 3 | 9.992770e+01 (2.544887e-01) | 9.794645e+01# (6.749397e+00) | 1.000303e+02 (2.020421e-01) | 9.425491e+01# (1.887090e+00) | 9.995196e+01 (2.218338e-01) |
| | 4 | 9.244139e+02 (3.316801e+00) | 8.974524e+02# (1.285704e+02) | 9.272970e+02 (2.893643e+00) | 8.519469e+02# (1.824213e+01) | 9.276510e+02 (2.419216e+00) |
| | 5 | 1.015545e+04 (5.247626e+01) | 7.528502e+03# (3.118251e+03) | 1.022660e+04 (2.444328e+01) | 9.147103e+03# (2.989196e+02) | 1.021265e+04 (2.425440e+01) |
| | 6 | 1.310595e+05 (5.984829e+02) | 5.753396e+04# (2.269538e+04) | 1.331408e+05 (4.343800e+02) | 1.178550e+05# (3.855927e+03) | 1.328084e+05 (6.917661e+02) |
| WFG6 | 2 | 8.360707e+00 (3.881634e-02) | 8.365132e+00 (4.216268e-02) | 8.373642e+00 (3.334034e-02) | 8.164502e+00# (1.036161e-01) | 8.349707e+00# (4.006040e-02) |
| | 3 | 7.316186e+01 (3.090747e-01) | 7.433975e+01 (3.131495e-01) | 7.356399e+01 (3.730537e-01) | 7.200035e+01# (6.485353e-01) | 7.364138e+01 (3.220770e-01) |
| | 4 | 7.349888e+02 (3.975988e+00) | 7.473567e+02 (3.402231e+00) | 7.396874e+02 (4.392577e+00) | 7.218089e+02# (7.685726e+00) | 7.422923e+02 (4.483313e+00) |
| | 5 | 8.496471e+03 (5.271866e+01) | 8.556716e+03 (9.691970e+02) | 8.640890e+03 (4.979948e+01) | 7.556842e+03# (1.664222e+02) | 8.661809e+03 (3.853133e+01) |
| | 6 | 1.083477e+05 (9.980675e+02) | 9.415101e+04# (2.883219e+04) | 1.167143e+05 (6.034739e+02) | 8.312614e+04# (1.675956e+03) | 1.168987e+05 (5.753055e+02) |

**Table 3: Mean and standard deviation (in parentheses) of the hypervolume indicator for the compared MOEAs and sIGD$^+$-MOEA in WFG2$^{-1}$ and WFG6$^{-1}$**

| MOP | Dim. | sIGD$^+$-MOEA | IGD$^+$-EMOA | NSGA-III | MOEA/D | MOMBI2 |
|---|---|---|---|---|---|---|
| WFG2$^{-1}$ | 2 | 5.937841e+01 (2.237740e-03) | 5.933772e+01# (1.725388e-02) | 5.938144e+01 (1.176128e-03) | 5.797012e+01# (7.237092e-02) | 5.905142e+01# (8.152131e-03) |
| | 3 | 7.319968e+02 (3.518163e-01) | 6.773068e+02# (7.783953e+00) | 7.256549e+02# (2.471515e+00) | 7.318071e+02# (5.137348e-01) | 7.277336e+02# (7.218694e-01) |
| | 4 | 1.040013e+04 (1.811214e+01) | 4.816314e+03# (6.745302e+01) | 1.018125e+04# (3.125945e+01) | 9.249223e+03# (8.345493e+02) | 1.004970e+04# (2.447182e+01) |
| | 5 | 1.640498e+05 (8.185932e+02) | 9.805288e+04# (4.411349e+04) | 1.470928e+05# (8.586496e+03) | 1.122933e+05# (1.197256e+04) | 1.499384e+05# (4.291788e+02) |
| | 6 | 2.855584e+06 (1.421240e+04) | 2.783331e+06# (2.624045e+04) | 2.132797e+06# (1.478385e+05) | 1.687099e+06# (1.866532e+05) | 2.503181e+06# (7.566149e+02) |
| WFG6$^{-1}$ | 2 | 5.825329e+01 (2.407529e-03) | 5.811072e+01# (3.129884e-02) | 5.824431e+01# (1.403821e-03) | 5.731344e+01# (7.849495e-02) | 5.765449e+01# (3.158869e-02) |
| | 3 | 7.552594e+02 (9.026264e-01) | 5.298722e+02# (2.874383e+01) | 7.467881e+02# (2.547384e+00) | 7.362416e+02# (1.543128e+00) | 7.514303e+02# (4.566291e-01) |
| | 4 | 1.185440e+04 (2.230257e+01) | 7.598649e+03# (2.210589e+01) | 1.130555e+04# (1.261387e+02) | 1.110350e+04# (8.380234e+01) | 1.127234e+04# (7.450687e+00) |
| | 5 | 2.119733e+05 (8.382179e+02) | 1.276462e+05# (9.209553e+02) | 1.941781e+05# (2.753116e+03) | 1.728454e+05# (1.224291e+03) | 1.890477e+05# (1.482334e+02) |
| | 6 | 4.085900e+06 (6.197265e+04) | 2.368114e+06# (9.756636e+03) | 3.694659e+06# (6.599968e+04) | 2.903169e+06# (2.763830e+04) | 3.213215e+06# (1.097736e+03) |

Since IGD$^+$-EMOA, NSGA-III, MOEA/D and MOMBI2 rely on the set of weight vectors in order to find intersection points with the Pareto front, they obtained, in general, uniformly distributed Pareto fronts. On the other hand, sIGD$^+$-MOEA relies on the s-energy indicator in order to obtain such distribution of solutions. However, the front generated by sIGD$^+$-MOEA is considerably well distributed, and it entirely covers the Pareto front surface.

Table 3 summarizes the HV results when tackling the minus versions of problems WFG2 and WFG6. From this table, it is evident that sIGD$^+$-MOEA produces the best results in all the test instances. Furthermore, as the number of objective functions increases, sIGD$^+$-MOEA presents a more considerable HV difference to the second best MOEA. In other words, the performance of our approach improves in many-objective optimization problems. Figure 1 shows the Pareto fronts related to the MOEAs in problem WFG6$^{-1}$, where it is possible to see that sIGD$^+$-MOEA generates uniformly distributed solutions, covering the Pareto front entirely. In contrast, the other MOEAs cannot produce uniformly distributed solutions due to the use of convex weight vectors and, in some cases, they cannot completely cover the Pareto front. On the basis of these results, it is possible to see that the performance of sIGD$^+$-MOEA is not strongly related to the shape of the Pareto front as is the case of the other MOEAs. Although sIGD$^+$-MOEA does not obtain the best results in the original WFG test problems, its performance is

**Figure 1: Pareto fronts produced by sIGD$^+$-MOEA and the considered MOEAs on problems WFG6 and WFG6$^{-1}$ for three objective functions. All fronts correspond to the median hypervolume values.**

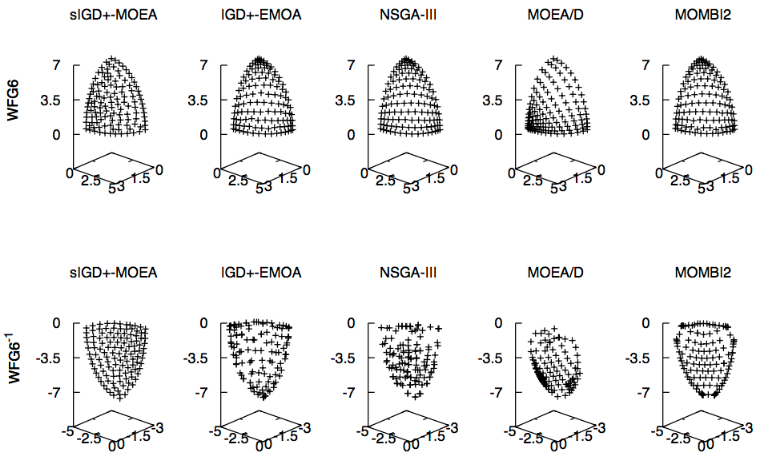


not very different from that of the best MOEA. Additionally, our approach does not get degrade when solving the minus versions of the considered MOPs as happens with the other MOEAs.

## 4 CONCLUSIONS AND FUTURE WORK

This paper presented a Many-Objective Evolutionary Algorithm that aims to be a more general optimizer. The new approach, called sIGD$^+$-MOEA, employs two density estimators based on the indicators IGD$^+$ and s-energy in order to improve both its convergence and diversity. The switching between the two indicator-based density estimators (IB-DEs) is done by statistically analyzing the quality of the population based on an approximation to the hypervolume indicator. sIGD$^+$-MOEA does not require a set of convex weight vectors in any of its mechanisms which allows it to solve MOPs having different Pareto front geometries. The experimental results have shown that our proposed approach is competitive with respect to NSGA-III, MOEA/D, MOMBI2 and IGD$^+$-EMOA in the original WFG test suite while it outperforms the adopted MOEAs in all the WFG$^{-1}$ problems when using the hypervolume indicator. There is still a lot of room for improvement, being the balance between IGD$^+$ and s-energy the most critical aspect to be analyzed. We have observed that S-ENERGY-DE usually accepts solutions that are not good in the Pareto dominance sense when tackling MaOPs. Hence, we have to improve the selection mechanism of the IB-DEs. Furthermore, the reference set of IGD$^+$ needs some refinement for MaOPs.

## ACKNOWLEDGMENTS

The first author acknowledges support from CINVESTAV-IPN and CONACyT to pursue graduate studies in Computer Science. The second author gratefully acknowledges support from CONACyT project no. 221551.

## REFERENCES

[1] Carlos A. Coello Coello, Gary B. Lamont, and David A. Van Veldhuizen. 2007. *Evolutionary Algorithms for Solving Multi-Objective Problems* (second ed.). Springer, New York. ISBN 978-0-387-33254-3.

[2] Kalyanmoy Deb and Himanshu Jain. 2014. An Evolutionary Many-Objective Optimization Algorithm Using Reference-Point-Based Nondominated Sorting Approach, Part I: Solving Problems With Box Constraints. *IEEE Transactions on Evolutionary Computation* 18, 4 (August 2014), 577–601.

[3] Jesús Guillermo Falcón-Cardona and Carlos A. Coello Coello. 2018. *sIGD$^+$-MOEA: towards a more general many-objective optimizer.* Technical Report 1. Department of Computer Science, CINVESTAV-IPN.

[4] D. P. Hardin and E. B. Saff. [n. d.]. Discretizing Manifolds via Minimum Energy Points. *Notices of the AMS* 51, 10 ([n. d.]), 1186–1194.

[5] Raquel Hernández Gómez and Carlos A. Coello Coello. 2015. Improved Metaheuristic Based on the $R2$ Indicator for Many-Objective Optimization. In *2015 Genetic and Evolutionary Computation Conference (GECCO 2015)*. ACM Press, Madrid, Spain, 679–686. ISBN 978-1-4503-3472-3.

[6] Simon Huband, Luigi Barone, Lyndon While, and Phil Hingston. 2005. A Scalable Multi-objective Test Problem Toolkit. In *Evolutionary Multi-Criterion Optimization. Third International Conference, EMO 2005*, Carlos A. Coello Coello, Arturo Hernández Aguirre, and Eckart Zitzler (Eds.). Springer. Lecture Notes in Computer Science Vol. 3410, Guanajuato, México, 280–295.

[7] Hisao Ishibuchi, Hiroyuki Masuda, Yuki Tanigaki, and Yusuke Nojima. 2015. Modified Distance Calculation in Generational Distance and Inverted Generational Distance. In *Evolutionary Multi-Criterion Optimization, 8th International Conference, EMO 2015*, António Gaspar-Cunha, Carlos Henggeler Antunes, and Carlos Coello Coello (Eds.). Springer. Lecture Notes in Computer Science Vol. 9019, Guimarães, Portugal, 110–125.

[8] Hisao Ishibuchi, Yu Setoguchi, Hiroyuki Masuda, and Yusuke Nojima. 2017. Performance of Decomposition-Based Many-Objective Algorithms Strongly Depends on Pareto Front Shapes. *Trans. Evol. Comp* 21, 2 (April 2017), 169–190.

[9] Hisao Ishibuchi, Noritaka Tsukamoto, and Yusuke Nojima. 2008. Evolutionary many-objective optimization: A short review. In *2008 Congress on Evolutionary Computation (CEC'2008)*. IEEE Service Center, Hong Kong, 2424–2431.

[10] Edgar Manoatl Lopez and Carlos A. Coello Coello. 2016. IGD$^+$-EMOA: A Multi-Objective Evolutionary Algorithm based on IGD$^+$. In *2016 IEEE Congress on Evolutionary Computation (CEC'2016)*. IEEE Press, Vancouver, Canada, 999–1006. ISBN 978-1-5090-0623-9.

[11] Qingfu Zhang and Hui Li. 2007. MOEA/D: A Multiobjective Evolutionary Algorithm Based on Decomposition. *IEEE Transactions on Evolutionary Computation* 11, 6 (December 2007), 712–731.

[12] Eckart Zitzler and Lothar Thiele. 1998. Multiobjective Optimization Using Evolutionary Algorithms—A Comparative Study. In *Parallel Problem Solving from Nature V*, A. E. Eiben (Ed.). Springer-Verlag, Amsterdam, 292–301.

[13] Eckart Zitzler, Lothar Thiele, Marco Laumanns, Carlos M. Fonseca, and Viviane Grunert da Fonseca. 2003. Performance Assessment of Multiobjective Optimizers: An Analysis and Review. *IEEE Transactions on Evolutionary Computation* 7, 2 (April 2003), 117–132.